Thermo-Induced Formation of Unimolecular and Multimolecular Micelles from Novel Double Hydrophilic Multiblock Copolymers of *N*,*N*-Dimethylacrylamide and *N*-Isopropylacrylamide

Yueming Zhou, Kunqiang Jiang, Qiliang Song, and Shiyong Liu*

Department of Polymer Science and Engineering, Joint Laboratory of Polymer Thin Films and Solution, Hefei National Laboratory for Physical Sciences at the Microscale, University of Science and Technology of China, Hefei, Anhui 230026, China

Received August 17, 2007. In Final Form: September 27, 2007

Two novel double hydrophilic multiblock copolymers of *N*,*N*-dimethylacrylamide and *N*-isopropylacrylamide, *m*-PDMA$_p$-PNIPAM$_q$, with varying degrees of polymerization (DPs) for PDMA and PNIPAM sequences (*p* and *q*) were synthesized via consecutive reversible addition−fragmentation chain transfer (RAFT) polymerizations using polytrithiocarbonate (***1***) as the chain transfer agent (Scheme 1), where PDMA is poly(*N*,*N*-dimethylacrylamide) and PNIPAM is poly(*N*-isopropylacrylamide). The DPs of PDMA and PNIPAM sequences were determined by ^{1}H NMR, and the block numbers, i.e., number of PDMA$_p$-PNIPAM$_q$ sequences (*n*), were obtained by comparing the molecular weights of multiblock copolymers to that of cleaved products as determined by gel permeation chromatography (GPC). *m*-PDMA$_{42}$-PNIPAM$_{37}$ and *m*-PDMA$_{105}$-PNIPAM$_{106}$ multiblock copolymers possess number-average molecular weights (M_n) of 4.62×10^4 and 9.53×10^4, respectively, and the polydispersities (M_w/M_n) are typically around 1.5. Block numbers of the obtained multiblock copolymers are ca. 4, which are considerably lower than the numbers of trithiocarbonate moieties per chain of ***1*** (∼20) and *m*-PDMA$_p$ precursors (∼6−7). PDMA homopolymer is water soluble to 100 °C, while PNIPAM has been well known to exhibit a lower critical solution temperature (LCST) at ca. 32 °C. In aqueous solution, *m*-PDMA$_{42}$-PNIPAM$_{37}$ and *m*-PDMA$_{105}$-PNIPAM$_{106}$ multiblock copolymers molecularly dissolve at room temperature, and their thermo-induced collapse and aggregation properties were characterized in detail by a combination of optical transmittance, fluorescence probe measurements, laser light scattering (LLS), and micro-differential scanning calorimetry (micro-DSC). It was found that chain lengths of PDMA and PNIPAM sequences exert dramatic effects on their aggregation behavior. *m*-PDMA$_{105}$-PNIPAM$_{106}$ multiblock copolymer behaves as protein-like polymers and exhibits intramolecular collapse upon heating, forming unimolecular flower-like micelles above the thermal phase transition temperature. On the other hand, *m*-PDMA$_{42}$-PNIPAM$_{37}$ multiblock copolymer exhibits collapse and intermolecular aggregation, forming associated multimolecular micelles at elevated temperatures. The intriguing aggregation behavior of this novel type of double hydrophilic multiblock copolymers argues well for their potential applications in many fields such as biomaterials and biomedicines.

Introduction

Significant advances have been made in the field of stimuli-responsive double hydrophilic block copolymers (DHBCs) within the past decade, mainly due to their potential applications in diverse fields such as drug delivery, catalysis, sensors, smart devices, and interface mediators.[1,2] Recent progress in this area includes preparation of DHBCs with novel chain architectures, such as pentablock,[3,4] Y-shaped,[5,6] H- or super H-shaped,[7] hyperbranched,[8] or miktoarm stars.[9]

For multiblock copolymers, the ordered alternation of two near-monodisperse but immiscible chain sequences endows them with fascinating aggregation properties in bulk and selective solvents.[10,11] In the latter case, a variety of mesophases with diverse morphologies such as micelles, vesicles, micellar rods, and helices have been observed for amphiphilic multiblock copolymers.[12−14] It is noteworthy that previous reports concerning the supramolecular self-assembly of DHBC with a multiblock architecture, *m*-(A-B)$_n$, have been rare. Existing examples mainly focused on the thermo-gelling behavior of multiblock copolymers prepared via the polycondensation of poly(ethylene oxide)-*b*-poly(propylene oxide)-*b*-poly(ethylene oxide) (PEO-*b*-PPO-*b*-PEO) triblock copolymers.[15−18] Cohn et al.[19] and Jeong et al.[20] found that the micellization of PEO-PPO multiblock copolymers leads to formation of much larger aggregates than that of the

* To whom correspondence should be addressed. E-mail: sliu@ustc.edu.cn.

(1) Rodriguez-Hernandez, J.; Checot, F.; Gnanou, Y.; Lecommandoux, S. *Prog. Polym. Sci.* **2005**, *30*, 691−724.
(2) Alarcon, C. D. H.; Pennadam, S.; Alexander, C. *Chem. Soc. Rev.* **2005**, *34*, 276−285.
(3) Determan, M. D.; Guo, L.; Thiyagarajan, P.; Mallapragada, S. K. *Langmuir* **2006**, *22*, 1469−1473.
(4) Determan, M. D.; Cox, J. P.; Seifert, S.; Thiyagarajan, P.; Mallapragada, S. K. *Polymer* **2005**, *46*, 6933−6946.
(5) Cai, Y.; Tang, Y.; Armes, S. P. *Macromolecules* **2004**, *37*, 9728−9737.
(6) Cai, Y.; Armes, S. P. *Macromolecules* **2005**, *38*, 271−279.
(7) Xu, J.; Ge, Z.; Zhu, Z.; Luo, S.; Liu, H.; Liu, S. *Macromolecules* **2006**, *39*, 8178−8185.
(8) Graham, S.; Rannard, S. P.; Cormack, P. A. G.; Sherrington, D. C. *J. Mater. Chem.* **2007**, *17*, 545−552.
(9) Ge, Z.; Cai, Y.; Yin, J.; Zhu, Z.; Rao, J.; Liu, S. *Langmuir* **2007**, *23*, 1114−1122.
(10) Nagata, Y.; Masuda, J.; Noro, A.; Cho, D. Y.; Takano, A.; Matsushita, Y. *Macromolecules* **2005**, *38*, 10220−10225.
(11) Quaglia, F.; Ostacolo, L.; Nese, G.; De Rosa, G.; La Rotonda, M. I.; Palumbo, R.; Maglio, G. *Macromol. Biosci.* **2005**, *5*, 945−954.
(12) Jia, Z. F.; Xu, X. W.; Fu, Q.; Huang, J. L. *J. Polym. Sci., Part A: Polym. Chem.* **2006**, *44*, 6071−6082.
(13) Sommerdijk, N. A. J. M.; Holder, S. J.; Hiorns, R. C.; Jones, R. G.; Nolte, R. J. M. *Macromolecules* **2000**, *33*, 8289−8294.
(14) Holder, S. J.; Hiorns, R. C.; Sommerdijk, N. A. J. M.; Williams, S. J.; Jones, R. G.; Nolte, R. J. M. *Chem. Commun.* **1998**, 1445−1446.
(15) Sosnik, A.; Cohn, D. *Biomaterials* **2005**, *26*, 349−357.
(16) Cohn, D.; Sosnik, A.; Levy, A. *Biomaterials* **2003**, *24*, 3707−3714.
(17) Cohn, D.; Sosnik, A.; Garty, S. *Biomacromolecules* **2005**, *6*, 1168−1175.
(18) Cohn, D.; Lando, G.; Sosnik, A.; Garty, S.; Levi, A. *Biomaterials* **2006**, *27*, 1718−1727.
(19) Cohn, D.; Sosnik, A.; Malal, R.; Zarka, R.; Garty, S.; Levy, A. *Polym. Adv. Technol.* **2007**, *9999*, n/a.
(20) Sun, K. H.; Sohn, Y. S.; Jeong, B. *Biomacromolecules* **2006**, *7*, 2871−2877.

10.1021/la702548h CCC: $37.00
Published on Web 11/21/2007

corresponding triblock copolymers. It should be noted that in the above examples the chain lengths of PEO and PPO sequences cannot be varied considerably because commercially available PEO-*b*-PPO-*b*-PEO, known as Pluronics or Poloxamers, etc., are typically employed as precursors.

On the other hand, it has been long predicted that, in dilute solutions of selective solvents, long multiblock copolymers could form unimolecular micelles via intramolecular collapse, which might possess conformations of flower-like or a flexible string of flowers.[21] However, to our knowledge, there is still no direct experimental evidence for formation of unimolecular micelles from linear and regular multiblock copolymers, probably due to the challenging nature of the synthesis of near-monodisperse samples with predetermined sequence lengths.

Generally, two main approaches have been developed for the synthesis of multiblock copolymers, *m*-(A-B)$_n$. The first one relies on the alternate addition two types of monomers (A and B) into a living polymerization system, such as living anionic polymerization.[22−24] This strategy obviously suffers from problems such as impurities introduced during each cycle of monomer addition and limited choice of monomer pairs. Alternatively, multiblock copolymers can also be prepared via intermolecular coupling of α,*ω*-functionalized block copolymers.[25−28] Due to the low concentration and poor accessibility of reactive end groups of diblock precursors, especially for those with relatively high molecular weights (>5000 Da), multiblock copolymers, *m*-(A-B)$_n$, with narrow polydispersity and large block numbers (*n*), i.e., the number of A-B sequences per chain, cannot be obtained.

Recently, a third approach has been applied to prepare multiblock copolymers in a more controlled and convenient way thanks to the advances achieved in controlled radical polymerizations. Endo et al.,[29,30] Pan et al.,[31] and Wang et al.[32,33] successfully prepared multiblock copolymers via consecutive reversible addition−fragmentation chain transfer (RAFT) polymerizations of two types of monomers utilizing poly or cyclic trithiocarbonates as the chain transfer agents. The chain length of each monomer sequence can be tuned by simply varying the ratio of monomers to trithiocarbonate moieties, and polydispersities of each monomer sequence and the final multiblock copolymer remain relatively narrow. Moreover, a variety of multiblock copolymers might be prepared because the RAFT technique is well known to be compatible with almost all conventional free radical polymerization monomers.

In conjunction with our recent research interests in stimuli-responsive DHBCs,[7,9,34−36] we further applied the above intriguing approach to the preparation of thermoresponsive double hydrophilic multiblock copolymers. Two acrylamido-based polymers, poly(*N*-isopropylacrylamide) (PNIPAM) and poly(*N*,*N*-dimethylacrylamide) (PDMA), were chosen as the building blocks. PNIPAM has been well known to exhibit a lower critical solution temperature (LCST) at ca. 32 °C in aqueous solution,[37] and PDMA is water-soluble up to 100 °C. Recently, McCormick et al.[38] synthesized diblock and triblock copolymers of DMA and NIPAM via consecutive RAFT polymerizations. They found that the chain architecture can play an important role on their thermo-responsive micellization behavior in aqueous solution. In contrast to diblock copolymers which exhibit multimolecular micellization, PDMA-*b*-PNIPAM-*b*-PDMA triblock copolymers with relatively short middle PNIPAM blocks do not form multimolecular micelles upon heating. We then feel that a direct comparison of the thermo-induced aggregation behavior between multiblock and diblock copolymers should be interesting.

Herein, we report on the synthesis of double hydrophilic multiblock copolymers of *N*,*N*-dimethylacrylamide and *N*-isopropylacrylamide, *m*-PDMA-PNIPAM, via RAFT polymerization using a polytrithiocarbonate (***1***) as the chain transfer agent (Scheme 1). ^{1}H NMR and GPC were employed to characterize the obtained multiblock copolymers. Moreover, UV−vis transmittance, fluorescence probe measurements, laser light scattering (LLS), and micro-differential scanning calorimetry (micro-DSC) were utilized to investigate the thermoresponsive aggregation behavior of *m*-PDMA-PNIPAM in aqueous solution. We successfully demonstrated that these multiblock copolymers can form unimolecular or multimolecular micelles, depending on the chain lengths of PDMA and PNIPAM sequences.

Experimental Section

Materials. *N*-Isopropylacrylamide (NIPAM, 97%, Tokyo Kasei Kagyo Co.) was purified by recrystallization from a mixture of benzene and *n*-hexane (1/3, v/v). *N*,*N*-Dimethylacrylamide (DMA, 98%, TCI) and styrene (St) were vacuum-distilled from CaH_2 and stored at −20 °C prior to use. 1,4-Dioxane was distilled over sodium/benzophenone. 2,2-Azoisobutyronitrile (AIBN) was recrystallized from ethanol. 1,4-Diphenylbutane and 2-(2-cyanopropyl) dithiobenzoate (CPDB) were synthesized according to literature procedures.[39,40] *N*-Bromosuccinimide (NBS), dibenzoyl peroxide (BPO), carbon tetrachloride, carbon disulfide (CS_2), and all other reagents were purchased from Sinopharm Chemical Reagent Co., Ltd. and used as received.

Sample Preparation. The general approach employed for the preparation of chain transfer agent, polytrithiocarbonate (***1***), and *m*-PDMA-PNIPAM multiblock copolymers is shown in Scheme 1. The target multiblock copolymer was synthesized via consecutive RAFT polymerization of DMA and NIPAM monomers.

Synthesis of 1,4-Dibromo-1,4-diphenylbutane (DBDPB). 1,4-Diphenylbutane (20.0 g, 0.095 mol), NBS (34.0 g, 0.191 mol), BPO (1.6 g, 6.61 mmol), and carbon tetrachloride (250 mL) were charged into a 500 mL round-bottom flask. After refluxing for 5 h, the reaction mixture was cooled to room temperature and then filtered. The filtrate was evaporated to dryness under reduced pressure. The obtained solids were recrystallized twice from THF/*n*-hexane (2/1 v/v). A 14.8 g amount of white needle crystals was obtained with a yield of 42%. ^{1}H NMR ($CDCl_3$, δ): 7.3 (m, 10H, *Ph*), 4.9 (t, 2H, PhC*H*Br), 2.1−2.5 (m, 4H, CHBrCH_2) (Figure 1a).

(21) Halperin, A. *Macromolecules* **1991**, *24*, 1418−1419.
(22) Masuda, J.; Takano, A.; Suzuki, J.; Nagata, Y.; Noro, A.; Hayashida, K.; Matsushita, Y. *Macromolecules* **2007**, *40*, 4023−4027.
(23) Spontak, R. J.; Smith, S. D. *J. Polym. Sci., Part B: Polym. Phys.* **2001**, *39*, 947−955.
(24) Eastwood, E. A.; Dadmun, M. D. *Macromolecules* **2001**, *34*, 740−747.
(25) Xie, H. Q.; Xie, D.; Chen, X. Y.; Guo, J. S. *J. Appl. Polym. Sci.* **2005**, *95*, 1295−1301.
(26) Loh, X. J.; Goh, S. H.; Li, J. *Biomacromolecules* **2007**, *8*, 585−593.
(27) Lee, J.; Bae, Y. H.; Sohn, Y. S.; Jeong, B. *Biomacromolecules* **2006**, *7*, 1729−1734.
(28) Hesna, G.; Thomas, M. L.; Monteiro, M. J.; Perrier, S. *J. Polym. Sci., Part A: Polym. Chem.* **2007**, *45*, 2334−2340.
(29) Motokucho, S.; Sudo, A.; Sanda, F.; Endo, T. *Chem. Commun.* **2002**, 1946−1947.
(30) Motokucho, S.; Sudo, A.; Endo, T. *J. Polym. Sci., Part A: Polym. Chem.* **2006**, *44*, 6324−6331.
(31) You, Y. Z.; Hong, C. Y.; Pan, C. Y. *Chem. Commun.* **2002**, 2800−2801.
(32) Zhang, L. S.; Wang, Q.; Lei, P.; Wang, X.; Wang, C.; Cai, L. *J. Polym. Sci., Part A: Polym. Chem.* **2007**, *45*, 2617−2623.
(33) Hong, J.; Wang, Q.; Fan, Z. Q. *Macromol. Rapid Commun.* **2006**, *27*, 57−62.
(34) Xu, J.; Luo, S.; Shi, W.; Liu, S. *Langmuir* **2006**, *22*, 989−997.
(35) Wang, D.; Yin, J.; Zhu, Z.; Ge, Z.; Liu, H.; Armes, S. P.; Liu, S. *Macromolecules* **2006**, *39*, 7378−7385.
(36) Ge, Z.; Xie, D.; Chen, D.; Jiang, X.; Zhang, Y.; Liu, H.; Liu, S. *Macromolecules* **2007**, *40*, 3538−3546.
(37) Schild, H. G. *Prog. Polym. Sci.* **1992**, *17*, 163−249.
(38) Convertine, A. J.; Lokitz, B. S.; Vasileva, Y.; Myrick, L. J.; Scales, C. W.; Lowe, A. B.; McCormick, C. L. *Macromolecules* **2006**, *39*, 1724−1730.
(39) Horning, E. E. *Organic Synthesis*; John Wiley & Sons Inc.: New York, 1955.
(40) Chiefari, J.; Chong, Y. K.; Ercole, F.; Krstina, J.; Jeffery, J.; Le, T. P. T.; Mayadunne, R. T. A.; Meijs, G. F.; Moad, C. L.; Moad, G.; Rizzardo, E.; Thang, S. H. *Macromolecules* **1998**, *31*, 5559−5562.

Scheme 1. Schematic Illustration of the Synthesis of Polytrithiocarbonate (*1*) and Multiblock Copolymers, *m*-PDMA$_p$-PNIPAM$_q$, by RAFT Polymerizations Using Polytrithiocarbonate (*1*) as the Chain Transfer Agent

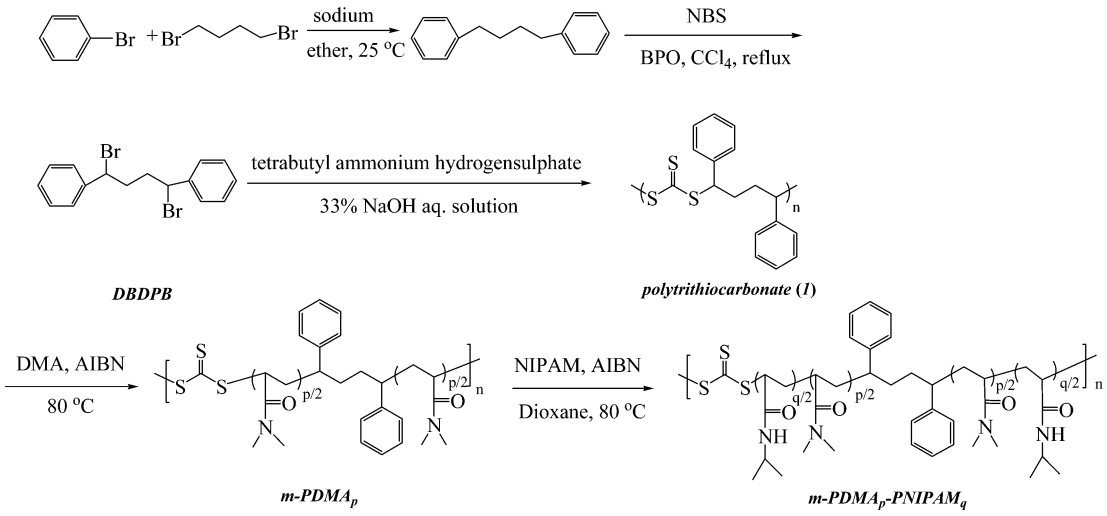

*Synthesis of Polytrithiocarbonate (**1**).* At ambient temperature, a mixture of CS_2 (20 mL) and 33% aqueous NaOH (20 mL) was stirred vigorously in a 100 mL round-bottom flask. Phase transfer catalyst, *n*-Bu_4NHSO_4 (0.2 g, 7 mol % relative to DBDPB), was then added, and the dispersion became blood red. After stirring for 10 min, DBDPB (3.0 g, 8.2 mmol) was introduced. The reaction mixture turned orange immediately. It was stirred for 24 h at room temperature. After standing for 1 h in a separation funnel, the CS_2 layer was collected and the aqueous layer was extracted with CS_2 (3×20 mL). The combined organic fractions were washed with water (2×20 mL). After drying over anhydrous Na_2SO_4 and filtration, the filtrate was concentrated and precipitated into an excess of methanol. The obtained product was further purified by washing with hot methanol (50 °C). Polytrithiocarbonate (***1***) was obtained as a yellow power (2.0 g; yield, ~80%). GPC analysis in DMF revealed a number-average molecular weight, M_n, of 6200 and a polydispersity, M_w/M_n, of 1.55.

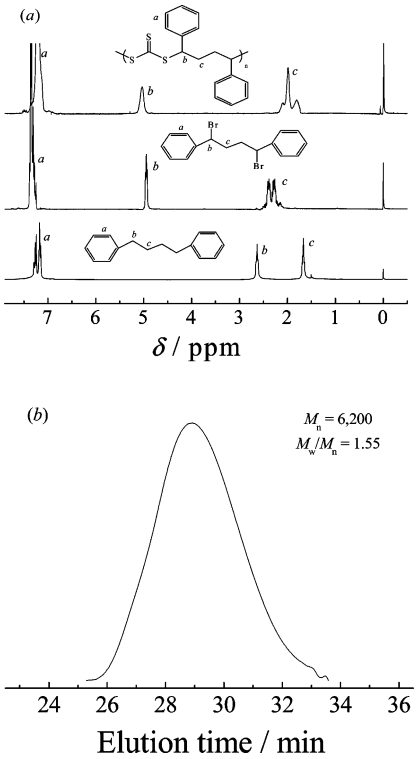

Figure 1. (a) ^{1}H NMR spectra of 1,4-diphenylbutane, 1,4-dibromo-1,4-diphenylbutane, and polytrithiocarbonate (***1***) in $CDCl_3$; (b) DMF GPC trace of the chain transfer agent, polytrithiocarbonate (***1***), employed for the subsequent synthesis of *m*-PDMA$_p$-PNIPAM$_q$ multiblock copolymers via RAFT processes.

*RAFT Polymerization of St using **1** as Chain Transfer Agent and Subsequent Cleavage.* To accurately identify the DP of the obtained polytrithiocarbonate ***1***, *m*-PS was prepared and subsequently cleaved.[31] The procedure was as follows. A glass ampule was charged with St (1.54 mL, 13.5 mmol), polytrithiocarbonate (***1***, 158 mg, 0.5 mmol trithiocarbonate moieties), and AIBN (4 mg, 25 μmol). The mixture was degassed by three freeze−pump−thaw cycles and flame-sealed under vacuum. The polymerization was conducted at 80 °C for 2 h. The viscous mixture was diluted with methylene chloride and then precipitated into an excess of methanol. The above purification cycle was repeated twice. The obtained slightly yellowish product was collected by filtration and dried in a vacuum oven for 12 h at room temperature. The molecular weight and molecular weight distribution of *m*-PS is characterized by GPC: $M_n = 29\,500$, $M_w/M_n = 1.50$.

For the subsequent cleavage of *m*-PS,[41] a 25 mL glass ampule was charged with AIBN (150 mg, 0.6 mmol), *m*-PS (50 mg), and 1,4-dioxane (10 mL). The mixture was degassed by two freeze−pump−thaw cycles and flamed-sealed under vacuum. After stirring at 80 °C for 4 h under stirring, the reaction mixture was cooled to room temperature and precipitated into an excess of methanol. The cleaved product was obtained as a white powder. GPC analysis revealed a number-average molecular weight, M_n, of 1700 and a polydispersity, M_w/M_n, of 1.09.

Synthesis of m-PDMA Precursors. A typical procedure for the synthesis of *m*-PDMA$_{105}$ precursor was as follows (Scheme 1). A glass ampule was charged with DMA (3.0 mL, 29.1 mmol), polytrithiocarbonate (***1***, 63.2 mg, 0.2 mmol trithiocarbonate moieties), and AIBN (1.6 mg, 10 μmol). The mixture was degassed by three freeze−pump−thaw cycles and flame-sealed under vacuum. The polymerization was conducted at 80 °C for 45 min. The viscous mixture was diluted with methylene chloride and then precipitated into anhydrous diethyl ether. The above purification cycle was repeated twice. The obtained slightly yellowish product was collected by filtration and dried in a vacuum oven for 12 h at room temperature. For the preparation of *m*-PDMA$_{42}$, the amount of ***1*** was varied while keeping the molar ratios of trithiocarbonate moieties to AIBN constant at 20:1. The polymerization conditions are summarized in Table 1.

Synthesis of m-PDMA-PNIPAM Multiblock Copolymers. In a typical run for the synthesis of *m*-PDMA$_{105}$-PNIPAM$_{106}$, a glass ampule was charged with NIPAM (0.5 g, 4.4 mmol), *m*-PDMA$_{105}$ macroRAFT agent (0.4 g, 38 μmol trithiocarbonate moieties), AIBN

(41) Perrier, S.; Takolpuckdee, P.; Mars, C. A. *Macromolecules* **2005**, *38*, 2033−2036.

Table 1. Summary of *m*-PDMA$_p$ Precursors and *m*-PDMA$_p$-PNIPAM$_q$ Multiblock Copolymers Prepared via RAFT Polymerizations

			uncleaved product[e]		cleaved product[f]		
samples	macroRAFT agent used	conversion (%)[d]	M_n (10^4)	M_w/M_n	M_n ($\times 10^4$)	M_w/M_n	block number (n)[g]
m-PDMA$_{42}$[a]	[***1***], 0.167 M[c]	69	6.39	1.43	0.89	1.09	7.2
m-PDMA$_{105}$[a]	[***1***], 0.067 M[c]	70	10.62	1.41	1.85	1.05	6.5
m-PDMA$_{42}$-PNIPAM$_{37}$[b]	*m*-PDMA$_{42}$	79	4.62	1.55	1.15	1.06	4.0
m-PDMA$_{105}$-PNIPAM$_{106}$[b]	*m*-PDMA$_{105}$	89	9.53	1.49	2.67	1.05	3.6

[a] The polymerization was conducted in bulk conditions: 3 mL DMA, 80 °C, ~45 min; the concentration of polytrithiocarbonate (***1***) was varied, while the molar ratios of trithiocarbonate moieties to AIBN were fixed at 20:1. [b] The polymerization was conducted in 1.5 mL 1,4-dioxane at 80 °C for ~50 min, 0.4 g *m*-PDMA$_p$ macroRAFT agent was used, and the molar ratios of AIBN to trithiocarbonate moieties were fixed at 1:10. [c] The concentration of trithiocarbonate moieties. [d] Monomer conversions determined by gravimetry. [e] Number-average molecular weights (M_n) and molecular weight distributions (M_w/M_n) of *m*-PDMA$_p$ and *m*-PDMA$_p$-PNIPAM$_q$ determined by GPC using DMF as eluents. [f] Number-average molecular weights (M_n) and molecular weight distributions (M_w/M_n) of the cleaved products after treating *m*-PDMA$_p$ and *m*-PDMA$_p$-PNIPAM$_q$ multiblock with an excess of AIBN at 80 °C in 1,4-dioxane. [g] Ratios of the molecular weights (M_n, GPC) of *m*-PDMA$_p$ or *m*-PDMA$_p$-PNIPAM$_q$ to that of the cleaved products.

(0.6 mg, 4 μmol), and 1,4-dioxane (1.5 mL). The homogeneous reaction mixture was degassed via three freeze−pump−thaw cycles and then flame-sealed under vacuum. The polymerization was conducted at 80 °C for 50 min. After quenching into liquid nitrogen to terminate the polymerization, the reaction mixture was diluted with methylene chloride and precipitated into an excess of anhydrous ethyl ether. The above purification cycle was repeated three times. The obtained yellowish product was dried overnight in a vacuum oven at room temperature. *m*-PDMA$_{42}$-PNPAM$_{37}$ multiblock copolymer was prepared following similar procedures, and the polymerization conditions are also summarized in Table 1.

Cleavage of m-PDMA and m-PDMA-PNIPAM. A typical run for cleavage of *m*-PDMA$_{105}$-PNIPAM$_{106}$ was as follows. A 25 mL glass ampule was charged with AIBN (16 mg, 0.1 mmol), *m*-PDMA$_{105}$-PNIPAM$_{106}$ (50 mg, 2 μmol trithiocarbonate moieties), and 1,4-dioxane (10 mL). The mixture was degassed by two freeze−pump−thaw cycles and flamed-sealed under vacuum. After stirring at 80 °C for 4 h, the reaction mixture was cooled to room temperature and precipitated into an excess of anhydrous diethyl ether. The cleaved product was obtained as a white powder.

Synthesis of PDMA-b-PNIPAM Diblock Copolymers. For comparison of the aggregation and micellization behavior between multiblock and corresponding diblock copolymers, PDMA-*b*-PNIPAM diblock copolymers were also synthesized by consecutive RAFT polymerizations of DMA and NIPAM monomers using CPDB as the chain transfer agent.

In a typical run, DMA (2 mL, 19.5 mmol), CPDB (26.5 mg, 120 μmol), AIBN (5 mg, 30 μmol), and 1,4-dioxane (2 mL) were charged into a 25 mL glass ampule. The mixture was degassed through three freeze−pump−thaw cycles. The ampule was then sealed under vacuum and immersed into an oil bath thermostated at 80 °C to conduct the polymerization. After 12 h, the ampule was plunged into liquid nitrogen to terminate the polymerization. Then the reaction mixture was diluted with methylene chloride and precipitated into an excess of anhydrous ethyl ether three times. The obtained red powders were dried overnight in a vacuum oven at room temperature. The molecular weight and molecular weight distribution of PDMA homopolymer was determined by GPC: M_n = 19 000, M_w/M_n = 1.10. The actual DP of PDMA was determined to be 110 by ^{1}H NMR analysis in $CDCl_3$. The obtained PDMA homopolymer was denoted as PDMA$_{110}$. Another PDMA homopolymer with a DP of 50, PDMA$_{50}$, was prepared according to similar procedures described above, and GPC analysis gave an M_n of 9100 and an M_w/M_n of 1.08.

Using PDMA$_{110}$ and PDMA$_{50}$ as macroRAFT agents, two PDMA-*b*-PNIPAM diblock copolymers were prepared by the RAFT polymerization of NIPAM monomers using similar RAFT protocols as described in the preparation of PDMA macroRAFT agent. The molecular weights and molecular weight distributions of PDMA$_{110}$-*b*-PNIPAM$_{112}$ (M_n = 26 700, M_w/M_n = 1.07) and PDMA$_{50}$-*b*-PNIPAM$_{45}$ (M_n = 12 900, M_w/M_n = 1.08) were determined by GPC analyses.

Characterization. *Nuclear Magnetic Resonance (NMR) Spectroscopy.* All ^{1}H NMR spectra were recorded in $CDCl_3$ or D_2O using a Bruker 300 MHz spectrometer.

Gel Permeation Chromatography (GPC). Molecular weights and molecular weight distributions were determined by gel permeation chromatography (GPC) equipped with a Waters 1515 pump and Waters 2414 differential refractive index detector (set at 30 °C). It used a series of three linear Styragel columns HT2, HT4, and HT5 at an oven temperature of 45 °C. The eluent was DMF at a flow rate of 1.0 mL/min. A series of low polydispersity polystyrene (PS) standards were employed for the GPC calibration.

UV−vis Transmittance Measurements. The optical transmittance of the aqueous solution was acquired on a Unico UV−vis 2802PCS spectrophotometer and measured at a wavelength of 600 nm using a thermostatically controlled cuvette.

Fluorescence Spectroscopy. Fluorescence spectra were recorded using a Shimadzu RF-5301PC spectrofluorometer. The temperature of the water-jacketed cell holder was controlled by a programmable circulation bath. The slit widths were set at 10.0 and 2.5 nm for excitation and emission, respectively. A calculated volume of pyrene solution in acetone was added into a volumetric flask followed by removing acetone under reduced pressure. Polymer solution was then added into the volumetric flask; pyrene concentration was fixed at 5×10^{-7} mol/L. All samples were sonicated for 2 h and then allowed to stand overnight before fluorescence measurements.

Laser Light Scattering (LLS). A commercial spectrometer (ALV/DLS/SLS-5022F) equipped with a multi-tau digital time correlator (ALV5000) and a cylindrical 22 mW UNIPHASE He−Ne laser (λ_0 = 632 nm) as the light source was employed for dynamic and static LLS measurements. Scattered light was collected at a fixed angle of 90° for a duration of ~10 min for micelles with an average hydrodynamic radius, $\langle R_h \rangle$, lower than ~100 nm. For larger aggregates such as those formed from *m*-PDMA$_{42}$-PNIPAM$_{37}$ in aqueous solution at elevated temperatures, scattering angles were varied from 15° to 50°; $\langle R_h \rangle$ values were obtained by extrapolation to zero angle. Distribution averages and particle size distributions were computed using cumulants analysis and CONTIN routines. All data were averaged over three measurements. The temperature was controlled by a programmable circulation bath. Each data point was obtained after the measured values were stable, which typically takes ~0.5 h.

In static LLS, we can obtain the weight-average molar mass (M_w) of aggregates in a dilute solution from the angular dependence of the excess absolute scattering intensity, known as Rayleigh ratio $R_{vv}(q)$. The specific refractive index increments (dn/dc) were determined by a precise differential refractometer at 632 nm. The molar mass of colloidal aggregates formed from *m*-PDMA$_{42}$-PNIPAM$_{37}$ was measured at only one concentration (1×10^{-4} g/mL), and extrapolation to zero concentration has not been conducted. Thus, the obtained molar mass should only be considered as apparent values, denoted as $M_{w,app}$.

Micro-Differential Scanning Calorimetry (micro-DSC) Characterization. Micro-DSC measurements were carried on a VP DSC from MicroCal. The volume of the sample cell was 0.509 mL. The reference cell was filled with deionized water. The sample solution with a concentration of 0.5 g/L was degassed at 25 °C for 0.5 h and equilibrated at 10 °C for 2 h before heating at a rate of 1.0 °C/min.

Results and Discussion

Synthesis of Multiblock Copolymers (*m*-PDMA-PNIPAM). The general approach employed for the preparation of *m*-PDMA-PNIPAM is shown in Scheme 1. The target multiblock copolymers were synthesized by consecutive RAFT polymerizations of DMA and NIPAM monomers using polytrithiocarbonate (***1***) as the chain transfer agent.

*Synthesis of Polytrithiocarbonate (**1**).* Multiblock copolymers can be obtained via RAFT polymerization utilizing cyclic or poly trithiocarbonate as the RAFT agent, and both of them can be prepared by reacting dihalide with an excess amount of CS_2 in the presence of base and phase-transfer catalyst. Leung et al.[42] reported that the yield of the main product strongly depends on the carbon chain length between two halide atoms on the dihalide. At a carbon chain length of 4, linear polytrithiocarbonate can be obtained with a yield up to ~88%. Starting from dihalide such as DBDPB, Wang et al.[33] reported a yield of cyclic trithiocarbonate of ~30%. In agreement with that reported by Leung et al.,[42] the main product is linear polytrithiocarbonate. In the current study, we chose linear polytrithiocarbonate (***1***) as the RAFT agent. The side product, cyclic trithiocarbonate, was readily removed by precipitation into methanol.

^{1}H NMR spectrum of polytrithiocarbonate ***1*** in $CDCl_3$ is shown in Figure 1a, and all characteristic signals of ***1*** are visible. It should be noted that after reacting DBDPB with CS_2 in the presence of NaOH and *n*-Bu_4NHSO_4, the resonance signal of methylene protons clearly shifted from 2.1−2.5 ppm in DPDPB to 1.6−2.2 ppm in ***1***; on the other hand, the resonance signal of the methine proton shifted from 4.9 ppm in DPDPB to 5.1 ppm in ***1***. The molecular weight and molecular weight distribution were determined by GPC, revealing a number-average molecular weight, M_n, of 6200 and a polydispersity, M_w/M_n, of 1.55. The GPC elution peak is symmetric but relatively broad, which is typical of the polycondensation product. As the molecular weight of the repeating unit is 316, the DP of ***1*** was estimated to be ~20.

Since GPC using PS as calibration standards can accurately report the M_n of PS samples, ***1*** was employed as the chain transfer agent for the RAFT polymerization of St. The obtained *m*-PS precursor and the cleaved product were subjected to GPC analysis. By comparing the molecular weight of *m*-PS (M_n = 29 500) with that of the cleaved product (M_n = 1700), the number of PS sequences per *m*-PS chain was calculated to be ~17, which generally agrees with the number of trithiocarbonate groups per chain of polytrithiocarbonate (***1***). Pan et al.[31] found that for the preparation of *m*-PS using a linear polytrithiocarbonate, the block number of the multiblock copolymer was close to the DP of polytrithiocarbonate precursor.

Synthesis of m-PDMA Precursors. In polytrithiocarbonate ***1*** the leaving groups linked to a trithiocarbonate moiety are benzyl groups with one methylene proton being substituted by an alkyl group, which is structurally similar to small molecule symmetric trithiocarbonates, e.g., dibenzyl trithiocarbonate,[43] employed in conventional RAFT polymerizations. We then expect that ***1*** can be employed to prepare polymers bearing a considerable number of trithiocarbonate moieties per chain; moreover, the sequence length between two neighboring trithiocarbonate should be controllable due to the 'living' nature of RAFT polymerization.

First, we employed polytrithiocarbonate (***1***) as the chain transfer agent for the RAFT polymerization of DMA monomer (Scheme 1). The obtained polymers were denoted as *m*-PDMA$_p$, where *p* stands for the average DP of PDMA sequence between two neighboring trithiocarbonate moieties. The molar ratios of AIBN to that of trithiocarbonate moieties were fixed at 1:20 to reduce the amount of homopolymer impurities and avoid the dramatic decrease of block numbers.

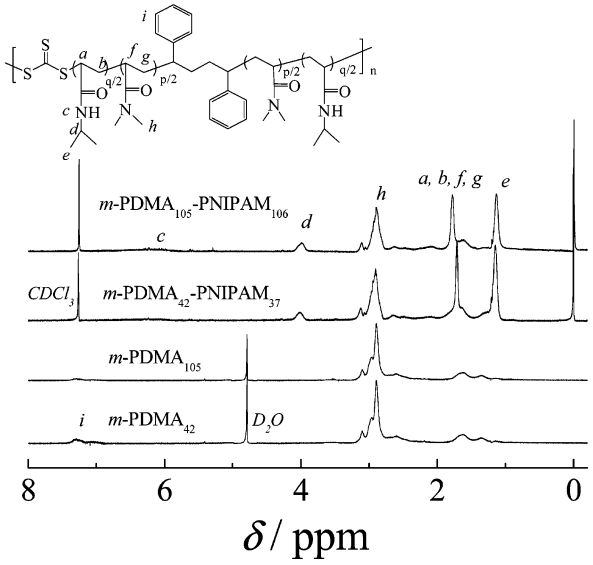

Figure 2. ^{1}H NMR spectra of *m*-PDMA$_p$ precursors and *m*-PDMA$_p$-PNIPAM$_q$ multiblock copolymers prepared by RAFT polymerizations.

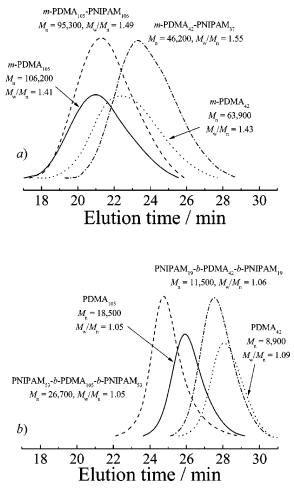

Figure 3. DMF GPC traces of (a) *m*-PDMA$_p$ precursors and *m*-PDMA$_p$-PNIPAM$_q$ multiblock copolymers, and (b) the corresponding products cleaved from *m*-PDMA$_p$ and *m*-PDMA$_p$-PNIPAM$_q$ by treating with an excess of AIBN at 80 °C in 1,4-dioxane.

Table 1 summarizes the polymerization conditions and structural parameters of *m*-PDMA and the cleaved product. The ^{1}H NMR spectrum of *m*-PDMA in D_2O is shown in Figure 2. The average PDMA sequence length (*p*) between two neighboring trithiocarbonate groups was calculated to be 105 by comparing the integrals due to the phenyl protons (peak *i*) of the trithiocarbonate moieties to that of the methyl protons (peak *h*) due to the PDMA sequences. The PDMA precursor was denoted as *m*-PDMA$_{105}$. The GPC traces of the obtained *m*-PDMA$_p$ precursors are shown in Figure 3a, and the structural parameters are summarized in Table 1. The M_w/M_n values of both *m*-PDMA samples were ~1.4.

From Table 1 and Figure 3a we can also tell that as the molar ratios of DMA monomer to that of the trithiocarbonate moiety increase, M_n values of *m*-PDMA precursors determined by GPC also increase. Taking *m*-PDMA$_{105}$ as an example, if we assume

(42) Leung, L. M.; Chan, W. H.; Leung, S. K. *J. Polym. Sci., Part A: Polym. Chem.* **1993**, *31*, 1799−1806.
(43) Tamami, B.; Kiasat, A. R. *J. Chem. Res. (S)* **1998**, 454−455.

that the number of PDMA sequences per *m*-PDMA$_{105}$ chain is equal to that of the number of trithiocarbonate moieties (∼20) of polytrithiocarbonate ***1***, the calculated M_n value for *m*-PDMA$_{105}$ should be $\sim 2.1 \times 10^5$. The M_n value determined by GPC for *m*-PDMA$_{105}$ is 1.06×10^5, which is much lower than that calculated. This indicates that the block number (*n*), i.e., the number of PDMA sequences per *m*-PDMA chain, is significantly less than 20.

To accurately determine the block number (*n*) per *m*-PDMA chain, the two *m*-PDMA samples were cleaved into individual PDMA sequences with the aid of an excess of AIBN.[41] Figure 3b shows the GPC traces of cleaved products. It is interesting to note that both elution peaks of cleaved PDMA sequences are symmetric and relatively monodisperse with typical M_w/M_n values of ∼1.1. This suggests that although the *m*-PDMA samples are relatively polydisperse, the growth of each PDMA sequence is still well controlled, exhibiting the living nature of typical RAFT polymerizations using small molecule chain transfer agent.

The block numbers (*n*) of both two *m*-PDMA samples were calculated from the ratio of the M_n of *m*-PDMA precursors to that of the cleaved products. Although GPC cannot give the accurate molecular weights of polymer samples, we expect the relative values should still be quite reliable. The block numbers are also summarized in Table 1, which are ∼6−7. Under similar conditions, the obtained *m*-PS possesses a block number of ∼17. Wang et al.[32,33] reported that by employing cyclic trithiocarbonates, the block number of *m*-poly(4-vinylpyridine) (*m*-P4VP) decreased more dramatically than that of *m*-PS with increasing polymerization time. For example, at the same monomer conversions (∼30%), the block numbers of *m*-PS and *m*-P4VP are 14 and 9, respectively. The mechanism leading to the prominent differences in block numbers for different types of monomers currently remains unclear.

Synthesis of m-PDMA-PNIPAM Multiblock Copolymers. These two *m*-PDMA precursors were then employed as the macroRAFT agents for the polymerization of NIPAM monomer, leading to formation of *m*-PDMA$_p$-PNIPAM$_q$, where *p* and *q* stand for the chain lengths (DP) of PDMA and PNIPAM sequences, respectively (Scheme 1). The polymerization conditions and structural parameters of multiblock copolymers are summarized in Table 1.

Figure 2 shows ^{1}H NMR spectra recorded for the multiblock copolymers. Besides the characteristic NMR resonance signals of PDMA sequences, we can clearly observe the characteristic PNIPAM signals at $\delta = 4.0$ and 1.1 ppm. The sequence length of PNIPAM can be calculated by comparing the integrated intensities due to PDMA (peak *h*) with that of PNIPAM (peak *e*). The two multiblock copolymer samples were then denoted as *m*-PDMA$_{105}$-PNIPAM$_{106}$ and *m*-PDMA$_{42}$-PNIPAM$_{37}$, respectively. It should be noted that although the DPs of PNIPAM and PDMA sequences are different for these two multiblock copolymers, the relative block compositions are similar.

Figure 3a shows the DMF GPC traces of *m*-PDMA$_p$-PNIPAM$_q$ multiblock copolymers. These GPC curves do not exhibit considerable shifts to higher molecular weights compared to that of *m*-PDMA$_p$ precursors, although ^{1}H NMR clearly reveals that PNIPAM sequences have been successfully incorporated (Figure 2). For *m*-PDMA$_{105}$-PNIPAM$_{106}$, the M_n value calculated by GPC (95 300) is even less than that of *m*-PDMA$_{105}$ (106 200). This must be due to the decreased block numbers (*n*) for the multiblock copolymers relative to that of *m*-PDMA precursors.

To verify the above hypothesis, the multiblock copolymers were cleaved in the presence of an excess of AIBN. From Figure 3b we can clearly tell that GPC traces of the cleaved products

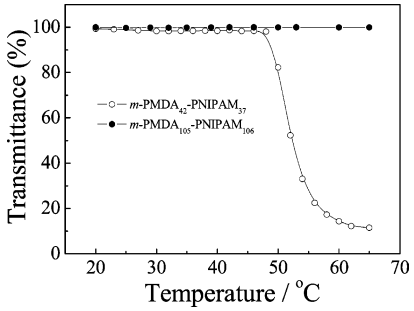

Figure 4. Temperature dependence of optical transmittance at 600 nm obtained for 0.5 g/L aqueous solutions of *m*-PDMA$_{42}$-PNIPAM$_{37}$ and *m*-PDMA$_{105}$-PNIPAM$_{106}$ multiblock copolymers.

from *m*-PDMA$_p$-PNIPAM$_q$ multiblock copolymers are both monomodal and symmetric. Most importantly, M_n values of the products cleaved from *m*-PDMA$_p$-PNIPAM$_q$ are systematically larger than that from *m*-PDMA$_p$ precursors. This strongly suggests NIPAM monomers have been successfully incorporated into the *m*-PDMA$_p$ chain bearing ∼6−7 trithiocarbonate groups, which agrees with the ^{1}H NMR result (Figure 2). On the basis of the well-accepted RAFT mechanism, the exact location of PNIPAM sequences in the multiblock copolymer should be on both sides of trithiocarbonate moieties, leading to the alternate arrangement of PDMA and PNIPAM sequences (Scheme 1).

Similar to that of *m*-PDMA precursors, the block numbers of multiblock copolymers can also be calculated by comparing their M_n values to those of the corresponding cleaved products (see Table 1). The numbers of PDMA$_p$-PNIPAM$_q$ sequences per chain are ∼4 for these two multiblock copolymers. In the order of polytrithiocarbonate (***1***), *m*-PDMA$_p$ precursors, and *m*-PDMA$_p$-PNIPAM$_q$, the average numbers of trithiocarbonate moieties per chain are decreasing. Similar conclusions were also reached by Wang et al.[32] The decrease of block numbers can be partially ascribed to the termination of growing multiblock polymer chains by radicals generated from the thermal decomposition of AIBN.

Aggregation Behavior of *m*-PDMA-PNIPAM. Generally, DHBCs containing PNIPAM blocks can self-assemble into micellar aggregates in aqueous solution at elevated temperatures due to the LCST phase behavior of PNIPAM at ca. 32 °C.[37] Previously studied examples involve varying chain topologies such as AB diblock,[38,44] ABA or BAB triblock,[38,45] star block copolymers,[34] and cylindrical brushes.[46] To our knowledge, *m*-PDMA$_p$-PNIPAM$_q$ synthesized in the current study represents the first example of double hydrophilic multiblock copolymers containing PNIPAM sequences. The aggregation behaviors of *m*-PDMA$_p$-PNIPAM$_q$ multiblock copolymers with block number of ∼4 were systematically investigated. Two diblock copolymers, PDMA$_{110}$-*b*-PNIPAM$_{112}$ and PDMA$_{50}$-*b*-PNIPAM$_{45}$, were also employed for comparison to explore the chain architectural effects (multiblock vs diblock) on the micellization properties of DHBCs.

Temperature-Dependent Optical Transmittance. Figure 4 shows the temperature dependence of optical transmittance at 600 nm obtained for 0.5 g/L aqueous solutions of *m*-PDMA$_{42}$-PNIPAM$_{37}$ and *m*-PDMA$_{105}$-PNIPAM$_{106}$. At a first glance, we are quite surprised that the two samples exhibit drastically different aggregation behavior in aqueous solution upon heating. For *m*-PDMA$_{42}$-PNIPAM$_{37}$, the transmittance starts to decrease dramatically at temperatures ≥ 48 °C. Above ∼60 °C, transmit-

(44) Cheng, C.; Schmidt, M.; Zhang, A.; Schluter, A. D. *Macromolecules* **2007**, *40*, 220−227.
(45) Li, C.; Tang, Y.; Armes, S. P.; Morris, C. J.; Rose, S. F.; Lloyd, A. W.; Lewis, A. L. *Biomacromolecules* **2005**, *6*, 994−999.
(46) Li, C.; Gunari, N.; Fischer, K.; Janshoff, A.; Schmidt, M. *Angew. Chem., Int. Ed.* **2004**, *43*, 1101−1104.

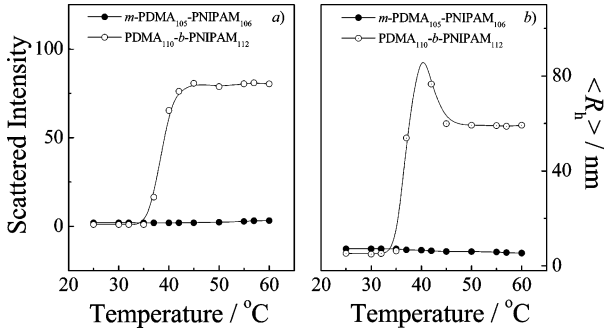

Figure 5. Temperature dependence of (a) scattered light intensity and (b) average hydrodynamic radius, $\langle R_h \rangle$, obtained for 0.5 g/L aqueous solutions of *m*-$PDMA_{105}$-$PNIPAM_{106}$ multiblock and $PDMA_{110}$-*b*-$PNIPAM_{112}$ diblock copolymers, respectively.

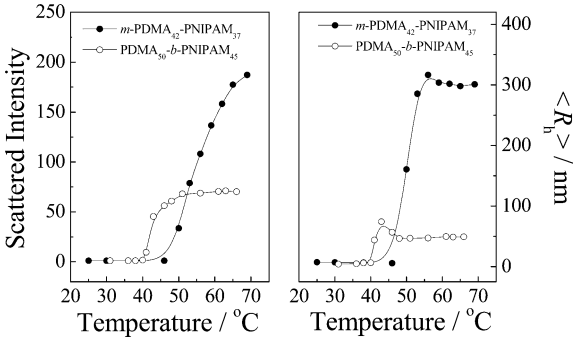

Figure 6. Temperature dependence of scattered light intensity and average hydrodynamic radius, $\langle R_h \rangle$, obtained for 0.1 g/L aqueous solution of *m*-$PDMA_{42}$-$PNIPAM_{37}$ multiblock and 0.5 g/L $PDMA_{50}$-*b*-$PNIPAM_{45}$ diblock copolymers.

tance becomes constant at ∼15%. The decrease in transmittance above 48 °C is ascribed to formation of aggregates due to the LCST phase behavior of PNIPAM sequences.

On the other hand, for 0.5 g/L aqueous solution of *m*-$PDMA_{105}$-$PNIPAM_{106}$, which has larger PDMA and PNIPAM sequence lengths but a comparable sequence length ratio compared to that of *m*-$PDMA_{42}$-$PNIPAM_{37}$, the transmittance does not change over the temperature range of 20−65 °C. Apparently, its does not exhibit extensive multimolecular aggregation during the heating process. Recently, McCormick et al.[38] reported that for PDMA-*b*-PNIPAM-*b*-PDMA triblock copolymers with relatively short PNIPAM block, multimolecular micellization did not occur upon heating above the LCST of PNIPAM block. However, in the current case, the different aggregation behavior between *m*-$PDMA_{105}$-$PNIPAM_{106}$ and *m*-$PDMA_{42}$-$PNIPAM_{37}$ possessing similar relative length ratios are quite perplexing.

Dynamic LLS Characterization. As temperature-dependent turbidimetry only reflects macroscopic changes of the aqueous solution of multiblock copolymers, LLS was used to characterize the aggregation behavior of multiblock copolymers in aqueous solution.

Figure 5 shows the temperature dependences of scattered light intensity and average hydrodynamic radius, $\langle R_h \rangle$, obtained for 0.5 g/L aqueous solutions of *m*-$PDMA_{105}$-$PNIPAM_{106}$ and $PDMA_{110}$-*b*-$PNIPAM_{112}$ during the heating process. At low temperatures, $PDMA_{110}$-*b*-$PNIPAM_{112}$ diblock copolymer molecularly dissolves with an average hydrodynamic radius, $\langle R_h \rangle$, of ∼5 nm and very low scattered intensity. Above ∼35 °C, both the scattered light intensity and $\langle R_h \rangle$ increase abruptly and reached plateau values at temperatures ≥ 45 °C (Figure 5), clearly revealing the multimolecular micellization. A bluish tinge characteristic of micellar solutions can be observed immediately upon heating. During heating, $\langle R_h \rangle$ exhibits a local maximum at ∼40 °C, decreases, and then remains at ∼60 nm at higher temperatures. Similar observations have also been reported by McCormick and co-workers for PDMA-*b*-PNIPAM block copolymers.[38]

On the other hand, LLS results are qualitatively different for the aqueous solution of *m*-$PDMA_{105}$-$PNIPAM_{106}$. Both the scattered light intensity and $\langle R_h \rangle$ remain almost unchanged in the temperature range 25−60 °C. A closer examination of Figure 5 indicates that the $\langle R_h \rangle$ values slightly decrease from ∼7 to ∼ 5 nm. However, this small change is basically within the measuring error of dynamic LLS. Since the scattered light intensity does not change upon heating, we conclude that the thermoresponsive aggregation above the LCST of PNIPAM sequences for *m*-$PDMA_{105}$-$PNIPAM_{106}$ occurs intramolecularly if the collapse of PNIPAM sequences occurs at elevated temperatures. It should be noted that the LLS results generally agree with those obtained from temperature-dependent turbidimetry, although the former can probe structural changes at a microscopic level.

Random copolymers with long correlation in sequence arrangement can exhibit similar unimolecular aggregation behavior as previously reported by Khokhlov and co-workers.[47−49] They defined these types of unimolecular aggregates as "protein-like" polymers, possessing hydrophobic units in the core and hydrophilic units in the shell. The intramolecular aggregation behavior of random copolymers was also reported by Yusa et al.[50] and McCormick et al.[51] The latter research group synthesized random or block copolymers of sodium 2-acrylamido-2-methylpropanesulfonate (AMPS) and sodium 3-acrylamido-3-methylbutanoate (AMBA), and their pH-induced aggregation behavior strongly depends on chain architectures.

For the multiblock copolymers in the current case, the sequence lengths also play an important role on their thermo-induced aggregation behavior in aqueous solution. Figure 6 depicts the temperature dependences of scattered light intensity and $\langle R_h \rangle$ obtained for aqueous solutions of *m*-$PDMA_{42}$-$PNIPAM_{37}$ (0.1 g/L) and $PDMA_{50}$-*b*-$PNIPAM_{45}$ (0.5 g/L). Upon heating, a bluish dispersion was obtained in both cases. As shown in Figure 4, heating the aqueous solution of *m*-$PDMA_{42}$-$PNIPAM_{37}$ at a concentration of 0.5 g/L leads to a turbid dispersion, so the LLS measurements of *m*-$PDMA_{42}$-$PNIPAM_{37}$ was conducted at a concentration of 0.1 g/L.

As can been seen from Figure 6, the micellization behavior of $PDMA_{50}$-*b*-$PNIPAM_{45}$ was quite similar to that of $PDMA_{110}$-*b*-$PNIPAM_{112}$. On the other hand, *m*-$PDMA_{42}$-$PNIPAM_{37}$ exhibits different aggregation properties compared to that of *m*-$PDMA_{105}$-$PNIPAM_{106}$. Both scattered light intensity and $\langle R_h \rangle$ dramatically increase above ∼46 °C for the former. This could be attributed to formation of larger aggregates above the LCST temperature of PNIPAM sequences. It should be noted that at 60 °C the formed aggregates exhibit an $\langle R_h \rangle$ of ∼300 nm.

The size of thermo-induced aggregates of *m*-$PDMA_{42}$-$PNIPAM_{37}$ (with block numbers *n* being ∼4) is quite large considering its chemical structure. If all polymer chains are in a stretched conformation, the radius of aggregates in solution should not exceed 79 × 4 × 0.25 nm = 79 nm if they possess well-defined core-corona microstructures typical of conventional

(47) Lozinsky, V. I.; Simenel, I. A.; Kulakova, V. K.; Kurskaya, E. A.; Babushkina, T. A.; Klimova, T. P.; Burova, T. V.; Dubovik, A. S.; Grinberg, V. Y.; Galaev, I. Y.; Mattiasson, B.; Khokhlov, A. R. *Macromolecules* **2003**, *36*, 7308−7323.
(48) Khokhlov, A. R.; Khalatur, P. G. *Physica A* **1998**, *249*, 253−261.
(49) Khokhlov, A. R.; Khalatur, P. G. *Phys. Rev. Lett.* **1999**, *82*, 3456−3459.
(50) Yusa, S.; Sakakibara, A. K.; Yamamoto, T.; Morishima, Y. *Macromolecules* **2002**, *35*, 5243−5249.
(51) Sumerlin, B. S.; Lowe, A. B.; Thomas, D. B.; McCormick, C. L. *Macromolecules* **2003**, *36*, 5982−5987.

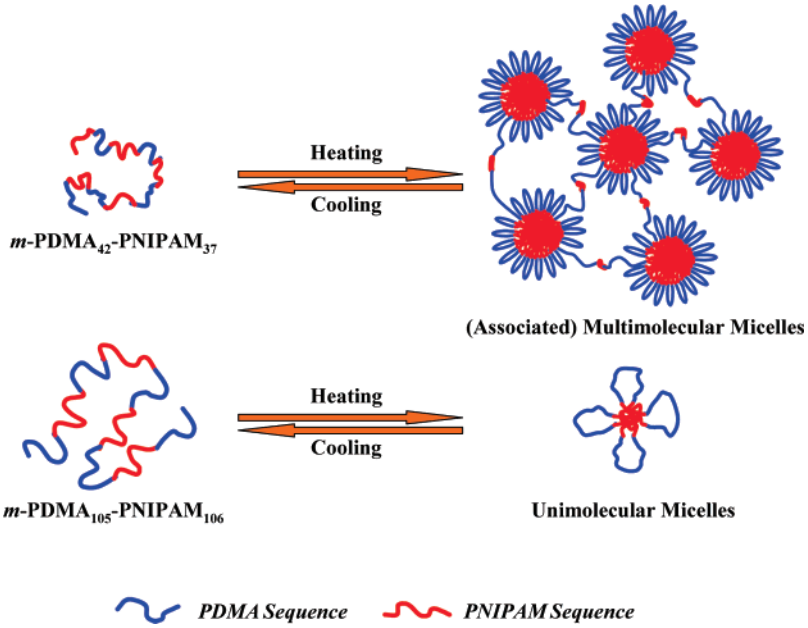

Figure 7. Schematic illustration of the formation of unimolecular and multimolecular micelles from *m*-PDMA$_p$-PNIPAM$_q$ multiblock copolymers with varying PDMA and PNIPAM sequence lengths.

micelles. We then tentatively speculate that *m*-PDMA$_{42}$-PNIPAM$_{37}$ chains initially aggregate and form multimolecular flower-like microstructures with PNIPAM sequences buried inside and stabilized by PDMA sequences at the periphery, and these flower-like micelles can be further bridged to each other by several multiblock copolymer chains with the PNIPAM sequences being located within cores of neighboring micelles. A schematic illustration is shown in Figure 7. Static LLS results indicate that the apparent weight-average molar mass, $M_{w,app}$, of the aggregates formed in aqueous solution (60 °C) of *m*-PDMA$_{42}$-PNIPAM$_{37}$ is 6.2 × 10^9 g/mol, and the average aggregation number (N_{agg}) per aggregates is calculated to be ∼1.19 × 10^5.

On the basis if the above LLS results, we tentatively conclude that *m*-PDMA$_{42}$-PNIPAM$_{37}$ forms associated multimolecular micelles while *m*-PDMA$_{105}$-PNIPAM$_{106}$ forms unimolecular flower-like micelles on heating their respective aqueous solutions (Figure 7). The thermo-induced intramolecular collapse of *m*-PDMA$_{105}$-PNIPAM$_{106}$ and intermolecular aggregation of *m*-PDMA$_{42}$-PNIPAM$_{37}$, i.e., formation of unimolecular or multimolecular flower-like micelles with hydrophobic domains consisting of PNIPAM sequences, was further confirmed by fluorescence probe and micro-DSC measurements as described in subsequent sections.

Fluorescence Probe Measurements. Information about the thermo-responsive micellization behavior of *m*-PDMA$_p$-PNIPAM$_q$ can also be derived from steady-state fluorescence technique employing pyrene as a probe. Typical emission spectra obtained for 0.5 g/L aqueous solution of *m*-PDMA$_{105}$-PNIPAM$_{106}$ (5.0 × 10^{-7} mol/L pyrene) at different temperatures are shown in Figure 8a. The emission spectra are characteristic of pyrene monomer fluorescence in specific microenvironments, where the ratio of the intensity of the first and third vibronic peaks, I_1/I_3, can be used to monitor formation of hydrophobic microdomains. If micelles form at elevated temperatures, the hydrophobic core consisting of PNIPAM sequences will tend to solubilize hydrophobic pyrene probes. A decrease in I_1/I_3 indicates the transfer of pyrene from a hydrophilic to a more hydrophobic microenvironment.

The I_1/I_3 ratio decreases with increasing temperatures. Figure 8b shows the temperature dependences of I_1/I_3 ratios obtained

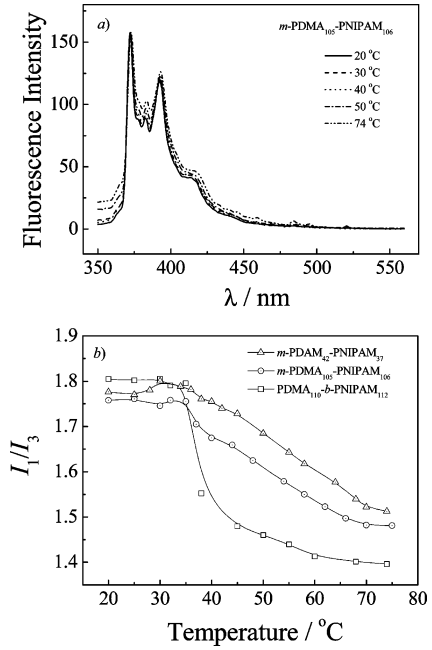

Figure 8. (a) Typical fluorescence emission spectra obtained for 0.5 g/L aqueous solution of *m*-PDMA$_{105}$-PNIPAM$_{106}$ at different temperatures; (b) plots of I_1/I_3 as a function of temperature obtained for PDMA$_{110}$-*b*-PNIPAM$_{112}$ diblock (0.5 g/L) and *m*-PDMA$_{105}$-PNIPAM$_{106}$ (0.5 g/L) and *m*-PDMA$_{42}$-PNIPAM$_{37}$ (0.1 g/L) multiblock copolymers. Pyrene concentration was fixed at 5.0 × 10^{-7} mol/L in all cases.

for aqueous solutions of *m*-PDMA$_{42}$-PNIPAM$_{37}$, *m*-PDMA$_{105}$-PNIPAM$_{106}$, and PDMA$_{110}$-*b*-PNIPAM$_{112}$. In the temperature range of 20−35 °C, I_1/I_3 ratios for all three samples are almost constant at ∼1.7−1.8, indicating that pyrene probes are located in hydrophilic environment and extensive thermoresponsive micellization does not take place. Upon further increasing the temperature, I_1/I_3 values decrease considerably in all three cases, indicating formation of hydrophobic domains consisting of PNIPAM sequences. It should be noted that the transition regions of the multiblock copolymers are much broader than that of the diblock copolymer.

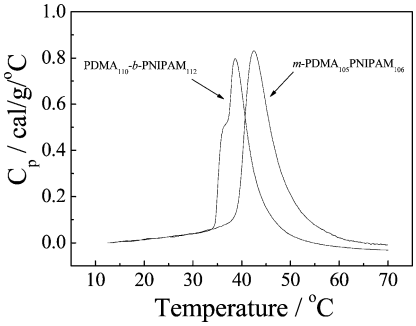

Figure 9. Temperature dependence of the specific heat capacity (C_p) obtained for 0.5 g/L aqueous solutions of *m*-PDMA$_{105}$-PNIPAM$_{106}$ and PDMA$_{110}$-*b*-PNIPAM$_{112}$. The heating rate was 1.0 °C/min.

For *m*-PDMA$_{42}$-PNIPAM$_{37}$ and PDMA$_{110}$-*b*-PNIPAM$_{112}$ copolymers, the intermolecular aggregation or formation of multimolecular aggregates can be apparently detected by visual inspection and supported by temperature-dependent turbidimetry and LLS measurements (Figures 4−6). On the other hand, for *m*-PDMA$_{105}$-PNIPAM$_{106}$ both turbidimetry and LLS results can only confirm that intermolecular aggregation does not occur. The decrease of I_1/I_3 at temperatures above 35 °C for the aqueous solution of *m*-PDMA$_{105}$-PNIPAM$_{106}$ can be clearly ascribed to formation of hydrophobic domains due to collapse of PNIPAM sequences (Figure 8b). Thus, unimolecular flower-like micelles with collapsed PNIPAM sequences as the core stabilized with PDMA sequences as the corona will form in the aqueous solution of *m*-PDMA$_{105}$-PNIPAM$_{106}$ upon heating.

Micro-DSC Characterization. Micro-DSC was further utilized to characterize the unimolecular aggregation of *m*-PDMA$_{105}$-PNIPAM$_{106}$ multiblock copolymer in aqueous solution. Figure 9 shows the temperature dependence of the specific heat capacity (C_p) for 0.5 g/L solutions of *m*-PDMA$_{105}$-PNIPAM$_{106}$ and PDMA$_{110}$-*b*-PNIPAM$_{112}$ during the heating cycle. Interestingly, a bimodal transition was observed for PDMA$_{110}$-*b*-PNIPAM$_{112}$ with one endothermic peak centered at 36.5 °C and the other at 38.5 °C. This is perhaps associated with the abnormal micellization ($\langle R_h \rangle$ maximum) as observed by dynamic LLS (Figure 5).

For the micro-DSC curve of *m*-PDMA$_{105}$-PNIPAM$_{106}$, only one endothermic peak can be observed, which can be obviously ascribed to the thermal phase transition of PNIPAM sequences. The onset temperature for the C_p increase is ∼38 °C, which is close to the inflection point (∼35 °C) in the I_1/I_3-T curve (Figure 8b). The enthalpy changes (ΔH) of the thermal phase transition of PDMA$_{110}$-*b*-PNIPAM$_{112}$ and *m*-PDMA$_{105}$-PNIPAM$_{106}$ were calculated to be 4.3 and 4.6 kJ/mol based on NIPAM repeating units, respectively. Thus, for both PDMA$_{110}$-*b*-PNIPAM$_{112}$ and *m*-PDMA$_{105}$-PNIPAM$_{106}$ in aqueous solution, increasing the temperature will break up hydrogen-bonding interactions between NIPAM residues and water molecules, leading to collapse of PNIPAM block or sequences and subsequent formation of multimolecular PNIPAM-core aggregates or unimolecular micelles for the former and latter multiblock copolymers, respectively.

On the basis of above intriguing results obtained from temperature-dependent turbidimetry, fluorescence probe measurements, LLS, and micro-DSC, we can conclude that *m*-PDMA$_{105}$-PNIPAM$_{106}$ can form unimolecular flower-like micelles in aqueous solution above the phase transition temperature of PNIPAM sequences while *m*-PDMA$_{42}$-PNIPAM$_{37}$ forms associated multimolecular flower-like micelles upon heating (Figure 7). Although these two multiblock copolymers possess similar length ratios of PDMA and PNIPAM sequences, the PDMA sequence length plays an important role. If it is too short, it cannot stabilize the collapsed PNIPAM sequences at elevated temperatures; thus, multimolecular flower-like micelles will form and then further bridge each other by multiblock copolymer chains located within different micelles to form larger associated aggregates.

To our knowledge, this represents the first observation of formation of unimolecular micelles from regular multiblock copolymers, as theoretically proposed by Halperin et al.[21] They predicted that long multiblock copolymer chains could form unimolecular micelles via intramolecular collapse, which possess conformations of flower-like or a flexible string of flowers. However, the techniques (LLS, micro-DSC, and fluorescence probe measurements) employed for characterization of unimolecular micelles in the current study cannot differentiate between these two conformations (flower-like or multiflower-like). It should also be noted that the block numbers of multiblock copolymers are quite low (∼4); thus, a direct comparison to previous theoretical predications[21] is inappropriate. The sequence-length-dependent aggregation behavior of multiblock copolymers is worthy of further theoretical considerations.

Conclusion

Double hydrophilic multiblock copolymers, *m*-PDMA-PNIPAM, were prepared via consecutive RAFT polymerizations using a polytrithiocarbonate as the chain transfer agent. The thermo-induced aggregation behavior of these multiblock copolymer solutions is complex. Unimolecular or multimolecular micelles can form upon heating the aqueous solutions of *m*-PDMA-PNIPAM multiblock copolymers with varying PDMA and PNIPAM sequence lengths. The interesting aggregation behavior of this novel type of double hydrophilic multiblock copolymers argues well for their potential applications in many fields such as biomaterials and biomedicines. Other properties of such multiblock copolymers, such as kinetics of multimolecular micellization and unimolecular collapse and thermo-induced gelation behavior, etc., are currently being explored in our lab.

Acknowledgment. This work was financially supported by an Outstanding Youth Fund (50425310) and research grants (20534020 and 20674079) from the National Natural Scientific Foundation of China (NNSFC), the "Bai Ren" Project and Special Grant (KJCX2-SW-H14) of the Chinese Academy of Sciences, and the Program for Changjiang Scholars and Innovative Research Team in University (PCSIRT).

LA702548H